Available online at www.sciencedirect.com

ScienceDirect

Publishing Services by Elsevier

International Journal of Naval Architecture and Ocean Engineering 8 (2016) 563−576
http://www.journals.elsevier.com/international-journal-of-naval-architecture-and-ocean-engineering/

A simulative method for evaluating the resistance of the flight deck's operational capability to the attack of anti-ship weapons

Fangqing Yang, Chao Wang*, Quanmi Liao, Sheng Huang

College of Shipbuilding Engineering, Harbin Engineering University, Harbin, China

Received 20 April 2016; accepted 30 May 2016
Available online 15 October 2016

Abstract

The flight deck of an aircraft carrier is relatively vulnerable compared to its hull, as the damage of some subsystems on the flight deck may cause the carrier losing its operational capability. Therefore, this work aims to represent a simulative method for evaluating the resistance of the flight deck's operational capability in the condition that the aircraft carrier is together with its strike group and the enemy uses the anti-ship missiles with the cluster warheads to attack. In the simulations, the susceptibility of the carrier and the vulnerability of the aircraft guarantee resources are gained. Then, with the help of the closed queuing network, the residual sortie generation rate can be solved, which reflects the flight deck's residual operational capability. The results have proven that the flight deck is of strong resistance to these attacks while it is very sensitive to the loss of some key aircraft guarantee resources.

Keywords: Aircraft carrier; Flight deck; Resistance; Operational capability; Sortie generation rate

1. Introduction

1.1. Background

The Carrier Air Wing (CVW) forms the most important part of the aircraft carrier strike group's operational capability. Thus, the sortie and recovery capability the carrier-borne aircrafts is one of the core technical indexes that the designers should concern (Michini and How, 2011; Zheng et al., 2013). Most of the aircraft guarantee work takes place on the flight deck (Ryan et al., 2011). However, if the flight deck is attacked by anti-ship weapons especially the missiles with cluster warheads, some key aircraft guarantee resources may be destroyed and this will weaken the flight deck's working ability greatly. If the aircraft carrier loses the sortie and recovery capability due to the damage of its flight deck, it has to retreat from the battle, even if its hull is intact. Therefore, the flight deck can be seen as one of the aircraft carrier's weak points.

With the help of the simulative method, the research work of this paper mainly aims to find out the flight deck's resistance to the anti-ship missiles with cluster warheads and the relationship between the damage of the flight deck and the aircraft carrier's residual operational capability.

1.2. Related literature and theory

1.2.1. The method for evaluating the warship's survivability

The survivability is an important part of a warship's combat effectiveness (Rains, 1994; Vassalos, 1999). To take the uncertainty into consideration, a warship's survivability contains 2 aspects and they are the susceptibility and the vulnerability (Ball, 1985). The former one concerns the probability that the warship being detected and hit by the enemy's weapons while the latter one concerns the damage degree caused by the enemy's weapons (Ball, 1994).

* Corresponding author.
E-mail address: wangchao806@hrbeu.edu.cn (C. Wang).
Peer review under responsibility of Society of Naval Architects of Korea.

http://dx.doi.org/10.1016/j.ijnaoe.2016.05.015

In this paper, the aircraft carrier is set to be protected by its carrier-borne aircrafts and other surface combat ships in the strike group. Before the enemy's anti-ship missiles have the chance to reach the aircraft carrier, they have to penetrate 3 defense zones respectively constructed by the intercept firepower of the carrier-borne aircrafts, the guided missile destroyers and the terminal defense weapons onboard the aircraft carrier (Sun, 2000). Thus, the susceptibility of the flight deck is mainly represented by the probability that the enemy's missiles escape and penetrate through the 3 defense zones and the positions that being hit by the warheads.

Traditionally, the vulnerability of a warship mainly includes the damage degree of the devices onboard and the floodability (Reese and Calvano, 1998; Said, 1995). In this paper, the vulnerability refers to the damage degree of the aircraft guarantee resources on the flight deck. There exist a number of methods and theories that can be applied to quantifying the combined influence of the subsystems' damage degree to the decline of the warship's operational capability (Wasmund, 2001), including the fault tree analysis (Shu et al., 2006) and the network theory (Albert et al., 2000; Albert and Barabási, 2002) which are being broadly used. In this paper, instead of other methods, the sortie generation rate is calculated to express the aircraft carrier's residual operational capability, since it is more ocular than any other indexes.

1.2.2. The method for calculating the sortie generation rate

The process of the carrier-borne aircrafts' sortie and recovery can be modeled with the closed queuing network (Dietz and Jerkins, 1997; Dastidar and Frazzoli, 2011), which should be non-preemptive and multi-class. The analytic solution of this closed queuing network can be gained by the Mean Value Analysis (MVA) (Bryant et al., 1984; Akyildiz and Gunter, 1988), in the condition that the model has to be properly simplified and leave out some constraints (Reiser, 1979). Therefore, though this method is fast and precise enough in some degree, it can't take all actual conditions into consideration. The simulative methods are conservative and slow, but much more precise than the analytic ones (Harris, 2002). As a result, in this paper, the Monte Carlo method is applied to solving the sortie generation rate as the residual operational capability.

2. The model of survivability evaluation for the flight deck

2.1. The susceptibility evaluation

The susceptibility evaluation in this paper aims to calculate the probabilities of every part of the aircraft carrier's flight deck and the aircraft guarantee resources on it to be hit by enemy's anti-ship warheads, when the whole strike group is performing an anti-air combat mission. The calculation contains 2 steps. One is to calculate the penetration probability of the enemy's anti-ship missiles when they fly across the defense system constructed by both the carrier-borne fighters and surface combat ships of the strike group. The other is the determination of the position where the warheads are to hit when these warheads break through the defense.

2.1.1. Calculation the penetration probability

The process of enemy's anti-ship missiles penetrating through the 3 defense zones of the strike group can be modeled by the queuing theory. 2 kinds of queuing systems are used to calculate the penetration probability.

(1) The mixed M/M/c/∞ queue with limited time for waiting

Since the depths of the outer and mid defense zones are relatively large, it takes a relatively long time for enemy's anti-ship missiles to fly through. Therefore, the penetration probability can be calculated with the help of the model of the mixed M/M/c/∞ queue with limited time for waiting. In this model, the process of penetration and interception can be taken as the customers waiting in a queue and being served by a number of servers. Therein, these incoming missiles are like the customers while the firepower passages of the strike group are like the servers. Thus, the situation that the enemy's anti-ship missiles don't encounter any interception during their flying across the current defense zone and succeed in penetrating caused by the saturation of the intercept firepower means the customer abandon the service and leave the queue due to waiting for too long.

For a certain defense zone, it is assumed that d_{f} and d_{c} respectively represent the far boundary and close boundary of the carrier-borne fighters or the regional air defense missiles' operational distance and the number of the intercept firepower passages is c. The incoming enemy's anti-ship missiles subject to the Poisson stream with the intensity of λ and their flying speed is v_{e}. If enemy's missiles succeed in penetration due to the saturation of the intercept firepower, the time that they spend in flying across the defense zone is t_{e}. Then, the penetration intensity of one single missile can be written as follows:

$$\nu = \frac{1}{t_e} = \frac{1}{\left(d_{\mathrm{f}} - d_{\mathrm{c}}\right)/v_{\mathrm{e}}} \tag{1}$$

The intercept operation generally includes detecting the targets, preparing to launch the interceptor missiles and the missiles flying towards the targets until them hitting or missing the targets. As t_{a} is assumed to be the service time, which means the time that needed to complete this operation, the average service rate of the intercept firepower in the current defense zone can be written as follows:

$$\mu = c\mu_{\mathrm{s}} = \frac{c}{t_{\mathrm{a}}} \tag{2}$$

In this equation, $\mu_{\mathrm{s}} = 1/t_{\mathrm{a}}$ means the average service rate of one single intercept firepower passage.

Let $N(t)$ be the number of incoming enemy's anti-ship missiles and the transition probability can be written as follows:

$$p_{ij}(\Delta t) = P\left\{N(t+\Delta t) = j|_{N(t)=i}\right\}$$

$p_{ij}(\Delta t)$ also satisfies the following equation:

$$p_{ij}(\Delta t)=\begin{cases}\lambda\Delta t+o(\Delta t), & j=i+1, i\geq 0\\ i\mu\Delta t+o(\Delta t), & j=i-1, i=1,2,\ldots,\mathrm{c}\\ [c\mu+(i-c)\nu]\Delta t+o(\Delta t), & j=i-1, i=c+1,c+2,\ldots\\ o(\Delta t), & |i-j|\geq 2\end{cases} \tag{3}$$

Then, $\{N(t), t\geq 0\}$ is the birth and death process of $\mathrm{E}=\{0,1,2,\ldots\}$, in which exists the following equation:

$$\lambda_i=\lambda,\quad i\geq 0;\quad \mu_i=\begin{cases}i\mu, & 1\leq i\leq c\\ c\mu+(i-c)\nu, & i>c\end{cases} \tag{4}$$

This birth and death process has the steady equilibrium solution and if let $t\to\infty$, the equilibrium equation set can be gained as follows:

$$\begin{cases}\lambda p_0=\mu p_1\\ (\lambda+i\mu)p_i=\lambda p_{i-1}+(i+1)\mu p_{i+1}, \quad i=1,2,\ldots,c-1\\ [\lambda+c\mu+(i-c)\nu]p_i=\lambda p_{i-1}+[c\mu+(i-c+1)\nu]p_{i+1}, \quad i=c,c+1,c+2,\ldots\end{cases} \tag{5}$$

Based on this equation, the expression of p_i can be educed as follows:

$$p_i=\begin{cases}\dfrac{\lambda^i}{i!\mu^i}p_0, & i=1,2,\ldots,c\\[2ex] \dfrac{\lambda^i}{c!\mu^c\prod\limits_{k=1}^{i-c}(c\mu+k\nu)}p_0, & i=c+1,c+2,\ldots\end{cases} \tag{6}$$

Considering that $\sum_{i=0}^{\infty}p_i=1,$, p_0 can be expressed as follows:

$$p_0=\frac{1}{\sum_{i=0}^{c}\frac{\lambda^i}{i!\mu^i}+\sum_{i=c+1}^{\infty}\frac{\lambda^i}{c!\mu^c\prod\limits_{k=1}^{i-c}(c\mu+k\nu)}} \tag{7}$$

Thus, the probabilities of the queuing system at every state can be easily calculated.

$$\overline{N}_q=E\left[N_q\right]=\sum_{i=c+1}^{\infty}(i-c)p_i \tag{8}$$

As the incoming intensity of the enemy's anti-ship missiles is λ and the penetration intensity of one single missile is ν, the penetration probability caused by the saturation of the intercept firepower can be expressed as follows:

$$P_e^{'}=\frac{\overline{N}_q\nu}{\lambda}=\frac{\nu}{\lambda}\left[\sum_{i=c+1}^{\infty}\frac{(i-c)\lambda^i}{c!\mu^c\prod\limits_{k=1}^{i-c}(c\mu+k\nu)}\right]p_0 \tag{9}$$

Considering that the hit rate of the intercept firepower cannot be as high as 100%, the enemy's anti-ship missiles encountered by the intercept firepower still has the chance to penetrate due to the interceptor missiles launched by the carrier-borne fighters or surface combat ships missing the target. Let p_{a} be the hit rate of every intercept firepower passage and considering all the factors above, the resultant penetration probability of the current defense zone can be written as follows:

$$P_e=P_e^{'}+\left(1-P_e^{'}\right)(1-p_{\mathrm{a}}) \tag{10}$$

After the intercept operation of the current defense zone, the incoming intensity of the enemy's anti-ship missiles decreases to $P_e\lambda$.

(2) The M/M/c/c queue with loss system

Different from the outer and mid defense zones, consisting of rapid-fire Gatling guns or other similar weapons, though the intercept firepower of the terminal defense zone has shorter response time and shooting period (usually shorter than 5s), the depth of this defense zone is much smaller. Additionally, as the enemy's anti-ship missiles will accelerate to a very high speed (faster than 3Ma) and change the trajectory, there isn't much time for the intercept firepower to perform the intercept operation. Once the intercept firepower passages are saturated at the same time the enemy's anti-ship missiles enter the current defense zone, the latter ones will successfully penetrate immediately. Thus, the combat process of penetration and interception in the terminal defense zone can be modeled by the M/M/c/c queue with loss system, which means the customers cannot bear any time for waiting if they don't receive the service immediately when they reach the service window.

It is assumed that the enemy's anti-ship missiles change its speed to v_{t}, so the time that these missiles spend flying through the current defense zone can be written as follows:

$$t_t=\frac{d_{\mathrm{f}}-d_{\mathrm{c}}}{v_{\mathrm{t}}} \tag{11}$$

As there is no customer in the queue, the queuing system has finite number of states and this number is $c+1$. So the equilibrium equation set of the birth and death process can be expressed as follows:

$$\begin{cases} \lambda p_0 = \mu p_1 \\ (\lambda + i\mu)p_i = \lambda p_{i-1} + (i+1)p_{i+1}, \quad i = 1, 2, \ldots, c-1 \\ c\mu p_c = \lambda p_{c-1} \end{cases} \tag{12}$$

Then, p_i can be educed as follows:

$$p_i = \frac{\lambda^i}{i!\mu^i} p_0, \quad i = 0, 1, 2, \ldots, c \tag{13}$$

Considering that $\sum_{i=0}^{\infty} p_i = 1$, p_0 can be expressed as follows:

$$p_0 = \frac{1}{\sum_{i=0}^{c} \frac{\lambda^i}{i!\mu^i}} \tag{14}$$

Due to the inference above, the penetration probability that the enemy's anti-ship missiles don't encounter the interception can be written as follows:

$$P_e^{'} = p_c = \frac{\lambda^c}{c!\mu^c} p_0 \tag{15}$$

In the terminal defense zone, the enemy's anti-ship missiles being intercepted also has the chance to escape and penetrate since the rapid-fire Gatling guns may miss the target either. For this kind of weapons, like the 730-Guns, the hit rate of one single gun can be determined by the empirical formula shown as follows:

$$p_a = 1 - \left(1 - \frac{p_{as}}{\omega}\right)^{n_g t_t} \tag{16}$$

In this equation, p_{as} is the hit rate of one single shot; ω is the average least number of the shells hit on every enemy's anti-ship missile to insure the destruction of the latter one; n_g is the firing rate of one single gun.

In summary, the resultant penetration probability of enemy's anti-ship missiles in the current defense zone can be expressed as follows:

$$P_e = P_e^{'} + \left(1 - P_e^{'}\right)(1 - p_a) \tag{17}$$

(3) The calculation of the penetration probability.

Let P_{e1}, P_{e2}, P_{e3} respectively represent the penetration probabilities when the enemy's anti-ship missiles successively fly through the outer, mid and terminal defense zones of the carrier strike group. Thus, the overall penetration probability for the enemy's anti-ship missiles' penetrating into the strike group and threatening the aircraft carrier can be represented in the form of product which is shown as follows:

$$P_e = P_{e1} \cdot P_{e2} \cdot P_{e3} \tag{18}$$

From the calculation model of P_{e1}~P_{e3} above, it can be inferred that among all the parameters, v_e and λ have the strongest influence on the value of P_e in the precondition that the military strength of the carrier strike group is certain. To analyze the degree of their influence, the calculating data are shown in Fig. 1, when the value of v_e and λ varies at a certain extent.

From the data points and curves in Fig. 1, it is very clear that P_e increases obviously with the increase of v_e. When λ is less than 14 min^{-1}, there are enough intercept firepower passages available to deal with the incoming enemy's anti-ship missiles, which causes that P_e hardly increases. When λ is larger than 14 min^{-1}, with the increase of the saturation probability of the intercept firepower, P_e increases much faster. Consequently, it can be inferred that improving the anti-ship missiles' flying speed and using the tactic of saturation attack will greatly add to the difficulty for the carrier strike group to defend.

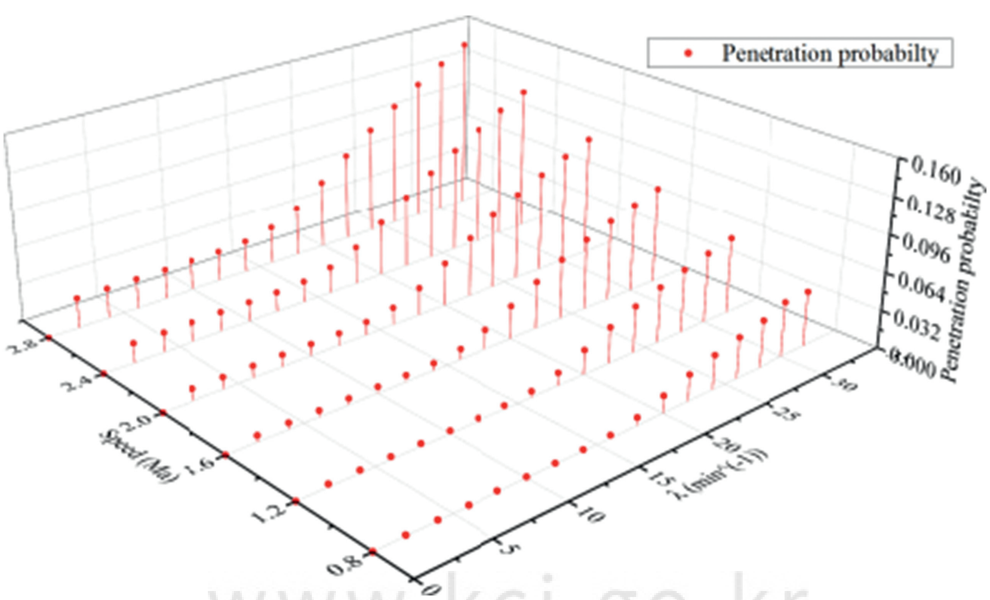

Fig. 1. The change of the penetration probability, P_e, with different values of v_e and λ.

2.1.2. Simulation of the hit positions

Once the enemy's anti-ship missiles escape from the interception and succeed in penetrating through the 3 defense zones of the strike group, they will have the chance to hit on the aircraft carrier's flight deck. As it is assumed that enemy equips their anti-ship missiles with the cluster warheads, the hit positions of both the missiles and the warheads carried by them should be considered and calculated.

(1) The flight deck-plate modeling

The concept of the flight deck-plate (FP) relates the workflows of the sortie and recovery operation with the general layout designs of the flight deck. The concrete method is that the whole flight deck of the aircraft carrier is divided into a quantity of squares with the same length of sides. These squares are numbered by their positions and any one of them is just a "flight deck-plate", which reflects the idea of discretization. When considering the position of any aircraft guarantee resources, there is no need to calculate its exact coordinates while knowing which FP it is in is enough. Thus, the amount of calculation is reduced. For example, when analyzing the survivability of a heavy aircraft carrier's flight deck (Norman, 1983), to ensure the computational accuracy while improving the efficiency, the coordinate system of *O-xy* can be established as shown in Fig. 2 and the flight deck can be divided into 80 FPs whose side is as long as 16 m.

Since the aircraft guarantee resources are distributed in all of the FPs, the degree of reduction of the aircraft carrier's operational capability will be different when the warheads hit the different FPs. When a specific FP is hit, whether the aircraft guarantee resources on it will be hit depends on a set of probabilities which are related to the shapes and sizes of these aircraft guarantee resources. What's more, the damage of some key FPs like the ones with the island or arresting wires on them will cause the operational capability greatly decline or even decline to 0.

(2) The hit positions of the anti-ship missiles

It is assumed that the position that every anti-ship missile aims at is the coordinate origin in Fig. 2 and the actual hit position obeys the 2-dimensional normal distribution taking the coordinate origin as central. The probability density function can be expressed as follows:

$$f(x,y)=\frac{1}{2\pi\sigma_x\sigma_y\sqrt{1-r^2}}\exp\left(-\frac{1}{2(1-r^2)}\left[\frac{x^2}{\sigma_x{}^2}-\frac{2rxy}{\sigma_x\sigma_y}+\frac{y^2}{\sigma_y{}^2}\right]\right) \tag{19}$$

In this equation, σ_x and σ_y respectively represent the standard deviations of x and y, and $\sigma_x > 0$, $\sigma_y > 0$; r represents the correlation coefficient of x and y, and $0 \le |r| < 1$.

As x and y are mutually independent, $r = 0$ and the Eq. (19) can be simplified as follows:

$$f(x,y)=\frac{1}{2\pi\sigma_x\sigma_y}\exp\left(-\frac{1}{2}\left[\frac{x^2}{\sigma_x{}^2}+\frac{y^2}{\sigma_y{}^2}\right]\right) \tag{20}$$

Thus, the actual hit positions of the anti-ship missiles represented by (x_{m}, y_{m}) can be calculated with the equation shown as follows:

$$\begin{cases} x_{\mathrm{m}}=\sigma_x\sqrt{-2\ln\nu_{\mathrm{m}1}}\cos(2\pi\nu_{\mathrm{m}2}) \\ y_{\mathrm{m}}=\sigma_y\sqrt{-2\ln\nu_{\mathrm{m}1}}\sin(2\pi\nu_{\mathrm{m}2}) \end{cases}, \nu_{\mathrm{m}1}=rand, \nu_{\mathrm{m}2}=rand \tag{21}$$

(3) The hit positions of the warheads

The number of warheads that every enemy's anti-ship missile carriers is N_{z}. When a missile is approaching the aircraft carrier, it will explode above the flight deck and throw out all the warheads. It is assumed that the hit positions of these warheads are independent and each of them obey the uniform distribution in the circular area which takes the missile's hit position as the circle center. The radius of this circular area is assumed to be R_{s}, so the hit positions of the warheads carried by a single missile can be expressed as follows:

$$\begin{cases} x_{\mathrm{z}}=x_{\mathrm{m}}+\nu_{\mathrm{z}1}R_{\mathrm{s}}\cos[(2\nu_{\mathrm{z}2}-1)\pi] \\ y_{\mathrm{z}}=y_{\mathrm{m}}+\nu_{\mathrm{z}1}R_{\mathrm{s}}\sin[(2\nu_{\mathrm{z}2}-1)\pi] \end{cases}, \nu_{\mathrm{z}1}=rand, \nu_{\mathrm{z}2}=rand \tag{22}$$

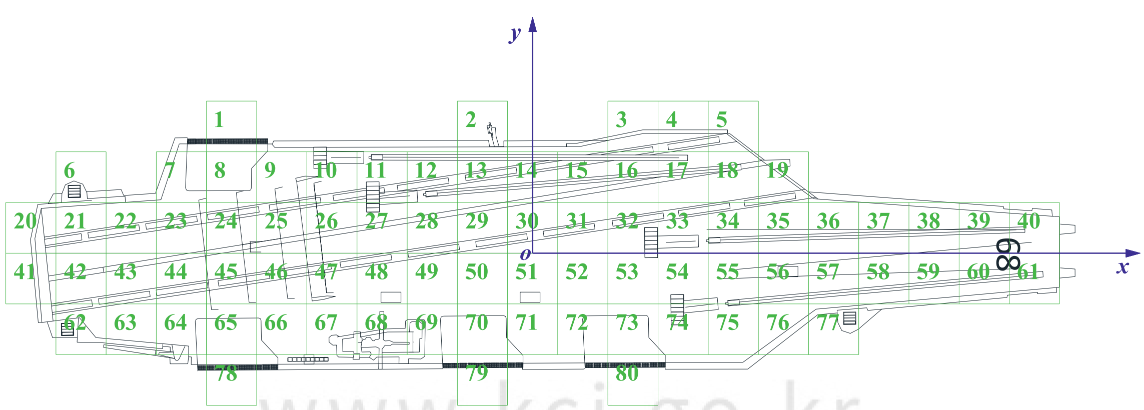

Fig. 2. The general view of the FPs of a heavy aircraft carrier.

As long as the hit positions of the warheads are gained, by contrast to the coordinate intervals of every FP, the FPs being hit and damaged can easily be found. Based on this, the damage degree of the aircraft guarantee resources on the flight deck can be solved with the help of vulnerability evaluation method which will be presented in the following context.

2.2. The vulnerability evaluation

The vulnerability evaluation in this paper mainly considers the survivability of the aircraft guarantee resources and the residual effectiveness of every workflow of the sortie and recovery operations on the flight deck. The workflows of the sortie and recovery operations for the carrier-borne aircrafts includes landing, fault checking, maintaining, refueling, relocating, rearming, catapulting to launch, and performing military tasks. To complete any of these workflows, multiple kinds of aircraft guarantee resources will be employed. Thus, the damage of the aircraft guarantee resources will weaken the effectiveness of the workflows of the sortie and recovery operations. All of the aircraft guarantee resources on the flight deck and their identifiers are shown in the following table.

2.2.1. The residual functions of the aircraft guarantee resources

The concept of insurance degree is applied to quantificationally representing the residual functions of the aircraft guarantee resources when the flight deck is hit by enemy's warheads. The value of an insurance degree is between 0 and 1, where 0 means totally destroyed while 1 means intact. Considering the concrete conditions of these aircraft guarantee resources in Table 1, the insurance degree of them will be calculated with different forms of functions.

(1) The "0−1" damage type

Some special devices on the flight deck are weakly protected while their physical constructions are complicated. Thus, once any one of them is hit by a single enemy's warhead, it will completely lose its working ability and the insurance degree will decline to 0. This kind of aircraft guarantee resources includes the catapults, arresting wires, flight elevators, optical landing assistant device, landing assistant radar and jet blast deflectors. Their insurance degree functions can be expressed as follows:

$$s_i(x) = \begin{cases} 0, & n \geq 1 \\ 1, & n = 0 \end{cases}, \quad i = 1, 2, \ldots, 12, 15, 16, 38, 39, \ldots, 41 \tag{23}$$

In this equation, n represents the number of enemy's warheads that hit the aircraft guarantee resource; the corner mark, i, corresponds to the identifiers in Table 1.

(2) The parking area and the island

The parking area covers almost 35% of the flight deck area, which is the main activity place of the carrier-borne aircrafts on the flight deck and is the work place of the refueling, rearming, maintaining and relocating teams. The island is the important command module of the aircraft carrier with many electronic instruments and command cabins in it. Both of these 2 kinds of aircraft guarantee take up relatively large area or volumes or have some protection. So they can sustain the hit from a number of warheads in some extent. Their insurance degree functions can be established by the drop half-ridge distribution function, expressed as follows:

$$s_i(n) = \begin{cases} 1, & n = 0 \\ \dfrac{1}{2} - \dfrac{1}{2}\sin\dfrac{\pi}{N_i}\left(n - \dfrac{N_i}{2}\right), & 0 < n < N_i, \quad i = 13, 17 \\ 0, & n \geq N_i \end{cases} \tag{24}$$

In this equation, N_{13} and N_{17} respectively represent the largest number of warheads that the parking area and the island can sustain being hit and their values are different.

(3) The landing strip

The landing strip locates in the angled area of the flight deck. Though it occupies quite a bit area, as the aircrafts are

Table 1
The aircraft guarantee resources on the flight deck.

Identifier	Aircraft guarantee resources	Identifier	Aircraft guarantee resources	Identifier	Aircraft guarantee resources
1	Catapult 1	15	Optical landing assistant device	29	Rearming team 1
2	Catapult 2	16	Landing assistant radar	30	Rearming team 2
3	Catapult 3	17	Island	31	Rearming team 3
4	Catapult 4	18	Refueling team 1	32	Rearming team 4
5	Arresting wire 1	19	Refueling team 2	33	Maintenance team 1
6	Arresting wire 2	20	Refueling team 3	34	Maintenance team 2
7	Arresting wire 3	21	Refueling team 4	35	Maintenance team 3
8	Arresting wire 4	22	Refueling team 5	36	Maintenance team 4
9	Flight elevator 1	23	Refueling team 6	37	Maintenance team 5
10	Flight elevator 2	24	Relocating team 1	38	Jet blast deflector 1
11	Flight elevator 3	25	Relocating team 2	39	Jet blast deflector 2
12	Flight elevator 4	26	Relocating team 3	40	Jet blast deflector 3
13	Parking area	27	Relocating team 4	41	Jet blast deflector 4
14	Landing strip	28	Relocating team 5		

very sensitive to the status of the landing strip when performing the landing operation, even a relatively small area of damage may lead to the unavailability of the landing strip. So, its insurance degree function can be written as follows:

$$s_{14}(n) = \begin{cases} 1, & n = 0 \\ 0.25, & n = 1 \\ 0, & n \geq 2 \end{cases} \tag{25}$$

(4) The guarantee teams on the flight deck

The refueling, rearming, maintaining or relocating teams usually consist of some support crews and the relevant guarantee devices. Their guarantee work takes place in the parking area, but their positions are not fixed. Thus, it is assumed that the probabilities that they being hit are the functions of s_{13}. As these guarantee teams lack of any kind protection, if any one of them is hit by a single enemy's warhead, its insurance degree will decline to 0. Their insurance degree functions can be expressed as follows:

$$s_i(n) = s_i(s_{13}(n)) = \begin{cases} 0, & k > s_{13}(n) \\ 1, & k \leq s_{13}(n) \end{cases}, \quad k = rand, \quad i = 18, 19, \ldots, 37 \tag{26}$$

(5) The carrier-borne aircrafts

When the enemy's warheads hit the flight deck, they will do damage to the carrier-borne aircrafts on the flight deck, too. In this paper, it is assumed that the number of the residual carrier-borne aircrafts is proportional to s_{13}, the value of the insurance degree of the parking area.

2.2.2. The residual effectiveness of the sortie and recovery operations

The residual effectiveness of the workflows of the sortie and recovery operations can also be represented by the insurance degree and it can be expressed as the functions of s_1~s_{41}. One thing is for sure that if the island is damage, the effectiveness of most of the workflows will be negatively affected.

(1) The landing

A conventional mono hull aircraft carrier usually has a single landing strip. Only a single carrier-borne aircraft is permitted to perform the landing operation at one time. The effectiveness of this workflow relates to the residual functions of the landing strip, arresting wires and the landing assistant radar. Thus, the insurance degree functions can be expressed as follows:

$$ss_1 = \frac{s_5 + s_6 + s_7 + s_8}{4} \cdot s_{14} \cdot \left(\frac{1}{4}s_{15} + \frac{3}{4}s_{16}\right) \cdot \left(\frac{1}{2} + \frac{1}{2}s_{17}\right) \tag{27}$$

(2) The fault checking

As the workload of the fault checking for carrier-borne aircrafts is relatively small and it also takes up little aircraft guarantee resources, it is assumed that the effectiveness of this workflow won't be affected by the status of the flight deck and its insurance degree is fixed to be 1.

$$ss_2 = 1 \tag{28}$$

(3) The maintaining

The effectiveness of maintaining operation is related to the status of not only the maintenance teams, but also the flight elevators, as in some particular situations the latter ones may transport the faulted or maintained aircrafts between the flight deck and the hanger. There are 5 maintenance teams on the flight deck and 5 aircrafts can be being maintained by them at one time. The insurance degree functions of the maintaining operations can be expressed as follows:

$$ss_{3i} = \left(\frac{1}{2} + \frac{s_9 + s_{10} + s_{11} + s_{12}}{8}\right) \cdot \left(\frac{1}{2} + \frac{1}{2}s_{17}\right) \cdot s_{i+32}, \quad i = 1, 2, \ldots, 5 \tag{29}$$

(4) The refueling, rearming and relocating

There are 6 refueling teams, 4 rearming teams and 5 relocating teams on the flight deck. Thus, the insurance degree functions of the related workflows can be expressed as follows:

$$ss_{4i} = \left(\frac{1}{2} + \frac{1}{2}s_{17}\right) \cdot s_{i+17}, \quad i = 1, 2, \ldots, 6 \tag{30}$$

$$ss_{6i} = \left(\frac{1}{2} + \frac{1}{2}s_{17}\right) \cdot s_{i+28}, \quad i = 1, 2, \ldots, 4 \tag{31}$$

$$ss_{7i} = ss_{5i} = \left(\frac{1}{2} + \frac{1}{2}s_{17}\right) \cdot s_{i+23}, \quad i = 1, 2, \ldots, 5 \tag{32}$$

(5) The catapulting

It should be noticed that a heavy aircraft usually has 4 catapults but only 3 of them can perform the workflow of catapulting at one time. The effectiveness of catapulting is related to the status of the jet blast deflector and catapults. Therefore, the insurance degree functions of the workflow of catapulting can be expressed as follows:

$$ss_{9i} = \left(\frac{1}{2} + \frac{1}{2}s_{17}\right) \cdot s_i \cdot s_{i+37}, \quad i = 1, 2, 3, 4 \tag{33}$$

3. The model of the sortie generation calculation

3.1. The closed queuing network of carrier-borne aircrafts sortie and recovery

Based on the analysis in former sections and some relevant references, the workflows of the carrier-borne aircrafts sortie and recovery operations can be simulated by a non-preemptive multi-class closed queuing network with shared service windows, which is shown in Fig. 3.

In this queuing network, the aircrafts on different tasks are set to be in different priority classes. The aircrafts in the same priority class receive the service according to the order that they arrived at the service station, while the aircraft in higher priority class receives the service in advance of those in lower priority class. The exceptional case is that the faulted aircrafts should perform the landing operation earlier than the intact ones. The 2 relocating service stations share the same relocating teams, which are the only shared service windows in this network. All the available carrier-borne aircrafts are usually divided into 3−5 squadrons and every squadron's timing for sortie is arranged in front of the combat.

3.2. The assumption of the service time

As a matter of experience, the service time is usually assumed to subject to the normal distribution or negative exponential distribution.

The service time of refueling, rearming and performing military tasks subjects to the normal distribution, shown as follows:

$$f(t) = \begin{cases} \lambda \cdot \exp(-\mu_s \cdot t), & t \geq 0 \\ 0, & t < 0 \end{cases} \tag{34}$$

The service time of other service stations subjects to the negative exponential distribution, shown as follows:

$$f(t) = \begin{cases} \dfrac{1}{\sigma_s \cdot \sqrt{2\pi}} \cdot \exp\left[-\dfrac{(t-\mu_s)^2}{2\sigma_s^2}\right], & t \geq 0 \\ 0, \quad t < 0 \end{cases} \tag{35}$$

In Eqs. (33) and (34), μ_s is the average service rate of any service station. While the residual effectiveness of the workflows is considered, the actual value of the average service rate can be expressed as follows:

$$\mu_s' = ss \cdot \mu_s \tag{36}$$

In this equation, *ss* is just the insurance degree which can be calculated with the vulnerability evaluation model in former sections.

In this closed queuing network, if any one of the service stations' effectiveness declines to 0, the customers as the aircrafts cannot circularly flow in the network. Thus, the sortie generation rate declines to 0, which causes the aircraft carrier lose the operational capability.

4. Case study and discussions

4.1. The input parameters

The strike group includes 1 heavy aircraft carrier and 6 destroyers.

The available aircrafts on the carrier's flight deck are 2 AEWs and 36 fighters. Each of the 2 AEWs uses the 1 + 15 triple-cycles. The fighters are divided into 3 squadrons and the 1 + 15 single-cycles are employed (Zheng et al., 2013; James and Harris, 2002), which means there are always 12 fighters ready for interception in the outer defense zone. Every fighter carries 3 short-range anti-air missiles as the interceptor missiles.

The destroyers equipped with the regional air defense missiles provide the intercept firepower of the mid defense zone. Each of the destroyers has 8 firepower passages. The 2

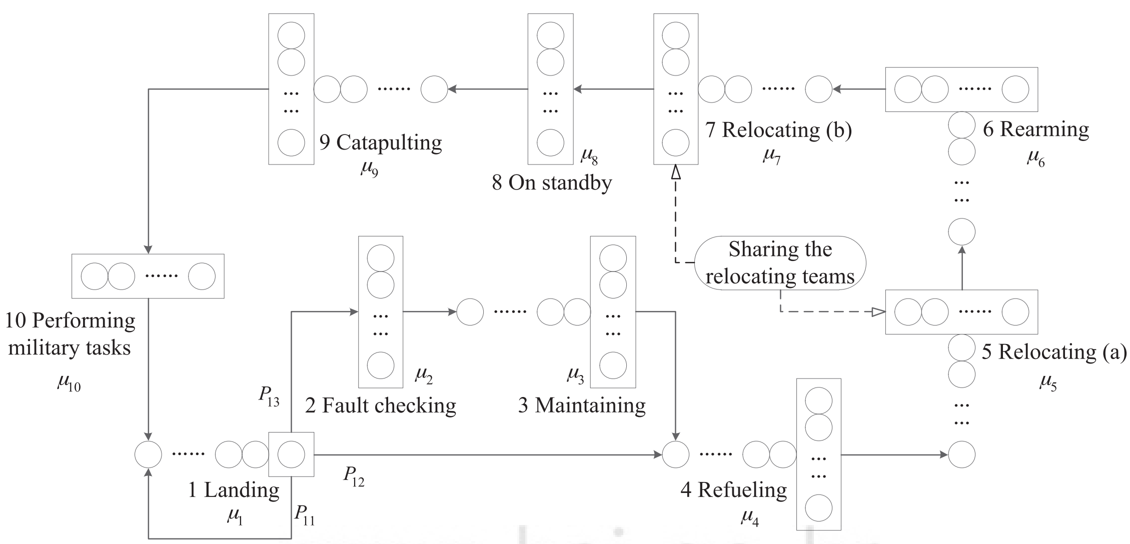

Fig. 3. Illustration of the closed queuing network of carrier-borne aircrafts sortie and recovery.

Table 2
Parameters of the defense zones.

Defense zone	Launch platform	Interceptor	c	d_f (km)	d_c (km)	t_a (min)	p_a/p_{as}	ω	n_g (min^{-1})
Outer	Carrier-borne fighters	Short-range anti-air missiles	36	400	185	75	0.95	\	\
Mid	Guided missile destroyers	Regional air defense missiles	48	185	5	1	0.6	\	\
Terminal	Rapid-fire guns	Armor-piercing shells	2	5	0	0.167	0.0094	2.67	4000

rapid-fire guns on the aircraft carrier provide the intercept firepower of the terminal defense zone.

Thus, the concrete settings of the 3 defense zones are shown in Table 2.

Based on the data in Angelyn's reports (1998a,b), the initial settings of the service stations when 1 + 15 cycle is employed are shown in Table 3. It is assumed that the Mean Time Between Failures (MTBF) of all the carrier-borne aircraft is 4 h.

The settings of the enemy's anti-ship missiles are shown in Table 4.

When calculating the sortie generation rate, the total work time is set to be 18 h. The situations of 4, 8, 12, 16, 24, 32, 48, 64, 96 and 128 enemy's anti-ship missiles incoming are considered. The Monte Carlo method (Cornebise, 2009; Andrieu, 2010) is applied to solving the result and the simulative computation will be circulated for 2000 times to calculate the sortie generation rate. To save the time expense, if the flight deck is intact in the current loop, instead of continuing the remaining calculation of this loop, based on the data collected in previous research, the sortie generation rate is estimated by generating a random number which obeys the normal distribution, N (120, 7.96).

4.2. The simulation result and discussion

4.2.1. The probability of being hit

To analyze the probability that the flight deck being hit of each simulative situation, Fig. 4 shows the frequency that at least one enemy's anti-ship missile succeeds in penetrating; Fig. 5 shows the detailed data of the number of the penetrated missiles. From Fig. 4, it can be inferred that the probability that the carrier being hit by at least one missile rises very quickly with the increase of the number of the incoming enemy's anti-ship missiles. Thanks to the intercept firepower of the 3 defense zones, this probability is relatively small when there are less than 8 missiles incoming. However, when there are more than 24 missiles incoming, the probability is at least as large as 80%.

From Fig. 5, it can be inferred that the average of the penetrated missiles is roughly in proportion to the number of incoming missiles. Thus, from both of these 2 figures, it can be concluded that the tactic of saturation attack is very effective in guarantee the penetration probability even the intercept

Table 3
Parameters of the service stations.

Identifier	Name	Number of service windows	μ_s (min^{-1})		σ_s (min^{-1})	
			AEW	Fighter	AEW	Fighter
1	Landing	1	53	53	\	\
2	Fault checking	$+\infty$	20	20	\	\
3	Maintaining	5	0.56	0.56	\	\
4	Refueling	6	3.33	2.4	0.4	0.4
5	Relocating (a)	5	20	20	\	\
6	Rearming	4	\	3	\	0.3
7	Relocating (b)	5	17	17	\	\
8	On standby	$+\infty$	\	\	\	\
9	Catapulting	3	30	30	\	\
10	Performing tasks	$+\infty$	0.23	0.48	0.5	0.5

Table 4
The parameters of the incoming enemy's anti-ship missiles.

v_e (Ma)	v_t (Ma)	λ (min^{-1})	σ_x (m)	σ_y (m)
2	6	24	60	20

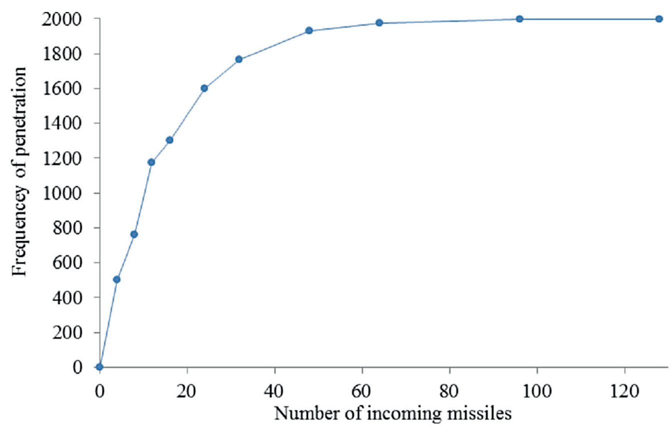

Fig. 4. The change of the frequency of penetration with different number of incoming missiles.

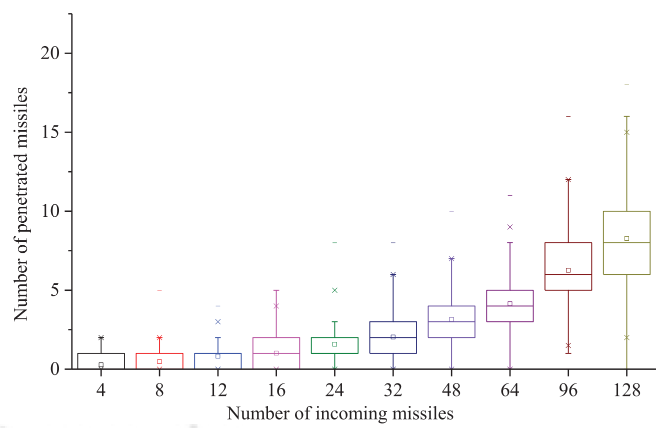

Fig. 5. The change of the number of penetrated missiles with different number of incoming missiles.

firepower of the strike group is thought to be rather strong. As the penetration probability rises, under the attack of the missiles with cluster warheads, the aircraft carrier's flight deck can hardly keep intact.

4.2.2. The damage of the service stations

In the closed queuing network of the carrier-borne aircrafts sortie and recovery, apart from the 3 service stations of fault checking, standing by and performing military tasks which don't rely on the aircraft guarantee resources, the frequencies of each service station being hit and being destroyed are shown in Figs 6—11.

From the blue round data points in Fig. 6, it can be seen that the 2 service stations of landing and maintaining are the most likely to be destroyed. This is mainly because that the area of the landing strip is relatively large, which adds to the probability of being hit by the warheads. At the same time, the insurance degree of the service station of maintaining is relevant to those of the 4 flight elevators, which also increases the probability of being hit. By contrast, though the area of the parking area is even larger than that of the landing strip and it occupies nearly 2/3 of the flight deck, as the positions of the refueling, rearming and relocation teams are not fixed, when the number of incoming enemy's anti-ship missiles is relatively small, the service stations of refueling, rearming and relocation are not so frequently to be hit by the warheads. With more missiles incoming, the gaps between the frequencies of each service station being hit become smaller. When the incoming

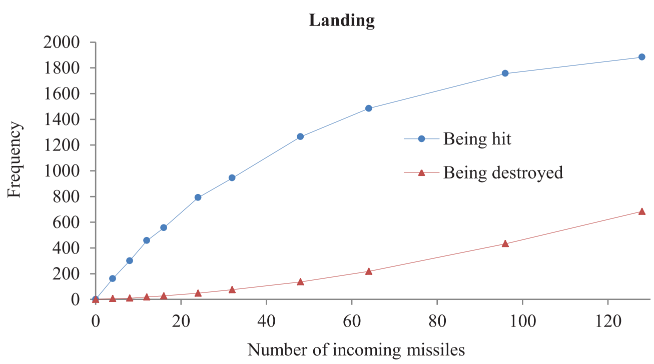

Fig. 6. The frequencies of landing station being hit and being destroyed.

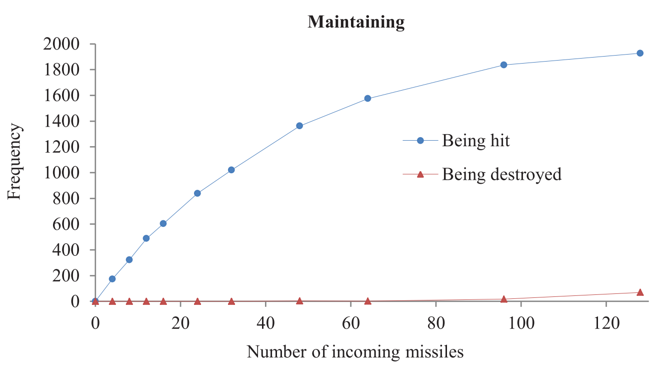

Fig. 7. The frequencies of maintaining station being hit and being destroyed.

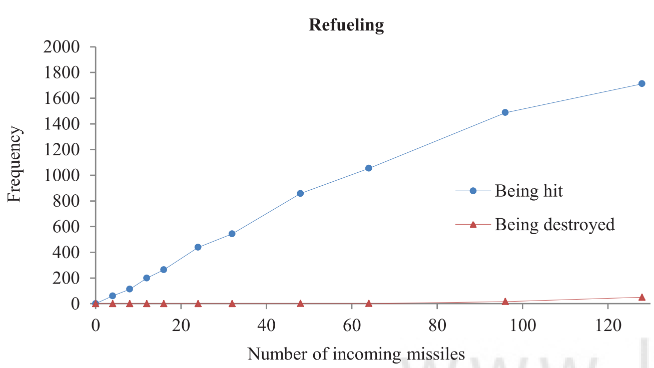

Fig. 8. The frequencies of refueling station being hit and being destroyed.

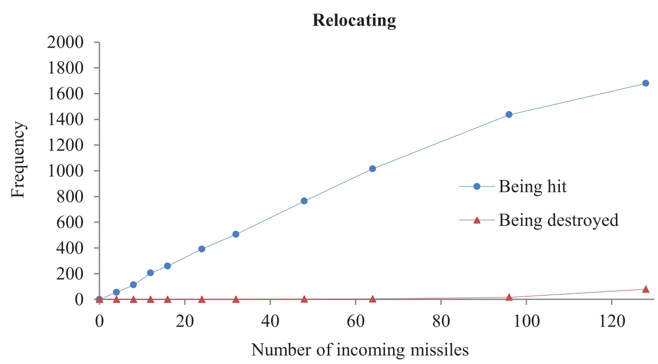

Fig. 9. The frequencies of relocating station being hit and being destroyed.

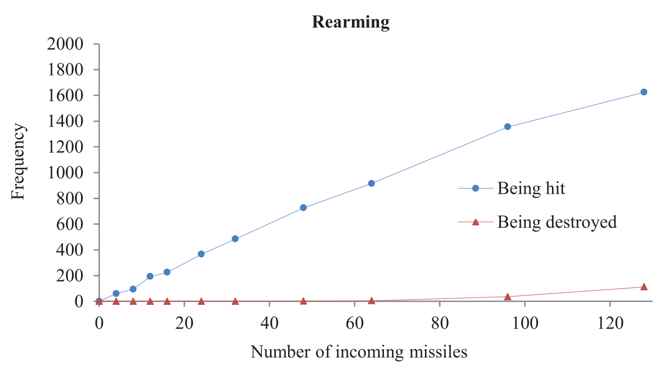

Fig. 10. The frequencies of rearming station being hit and being destroyed.

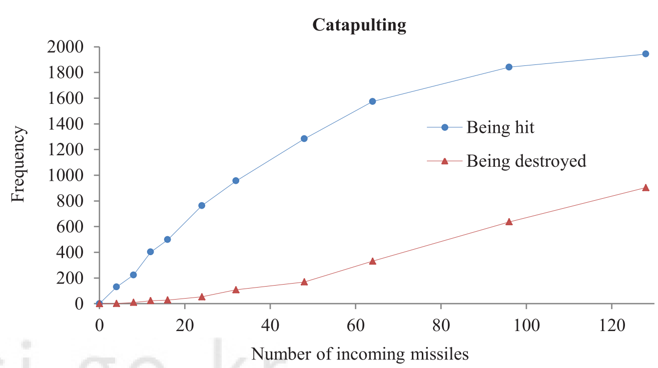

Fig. 11. The frequencies of catapulting station being hit and being destroyed.

enemy's missiles are more than 64, the frequencies of being hit are roughly in the same order of magnitude.

According to the red triangular data points in Fig. 6, the 2 service stations of landing and catapulting are the most likely to be destroyed. As any service station being destroyed and losing its insurance degree will cause the sortie generation rate declining to 0, it can be deduced that these 2 service stations are the weakness of the entire closed queuing network. Compared with them, other service stations have relatively more chances to survive during the combat. As long as the insurance degree of the parking area is larger than 0, the aircraft guarantee teams always have the activity space and still have some working abilities.

Furthermore, the concept of integrity is introduced to measure the damage degree of these 6 service stations and it can be calculated by the following equation:

$$D_I(i) = \frac{\sum_{j=1}^{M} \mu_s^{(i,j)}}{M\mu_s^{(i)}}, \; i = 1,3,4,5,6,7,9 \tag{37}$$

where the corner mark i indicates the ith service station and j indicates the jth service window of that service station; $\mu_s^{(i)}$ represents the service rate of the service windows in the ith service station which has M service windows in total, when the service station is intact; $\mu_s^{(i,j)}$ represents the service rate of the jth service window in the ith service station. The change of the degree of integrity with different number of incoming missiles is shown in Fig. 12—17.

The figures above indicate that the trends of the decline of these curves differ at a certain extent. The curves in Figs. 12 and 13 are similar and their decline trends are approximately linear. This is mainly because the insurance degrees of landing and maintaining service station are respectively related to that of the arresting wires and flight elevators, whose calculation modes are the same as Eq. (23). The curves in Figs. 14—16 are very close to each other too, as the insurance degrees of the aircraft guarantee teams are the function of that of the parking area, expressed as Eq. (26). When there are less than16 enemy's anti-ship missiles incoming, their insurance degrees decline very slow. This is mainly because the parking area is relatively large and only a few warheads hitting on it can hardly weaken its insurance degree. Comparatively speaking, the curve in Fig. 17 declines much faster and when there are

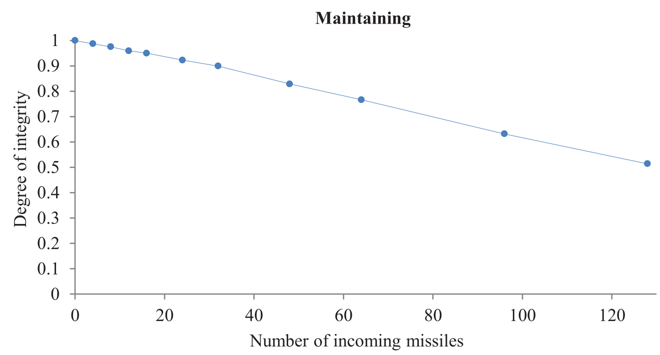

Fig. 13. The degree of integrity of maintaining service station.

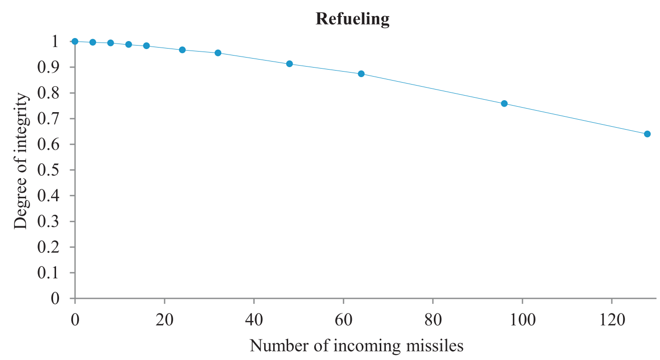

Fig. 14. The degree of integrity of refueling service station.

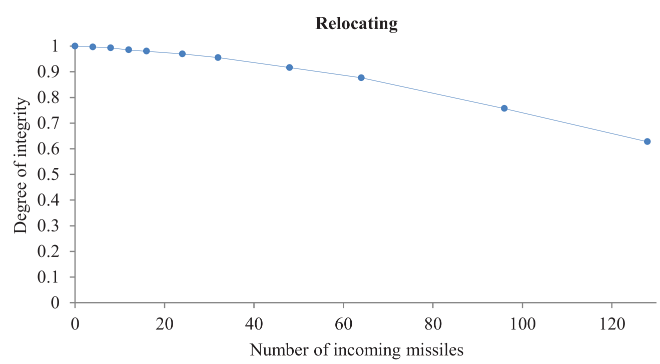

Fig. 15. The degree of integrity of relocating service station.

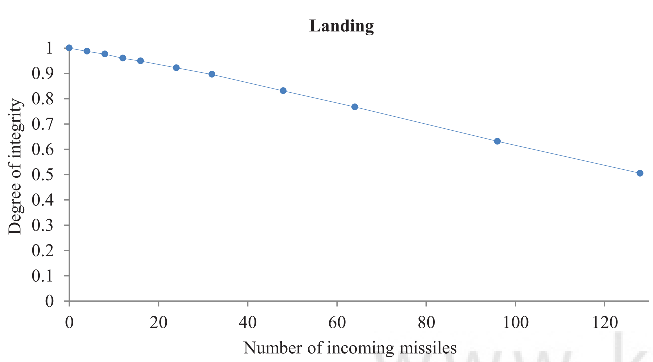

Fig. 12. The degree of integrity of landing service station.

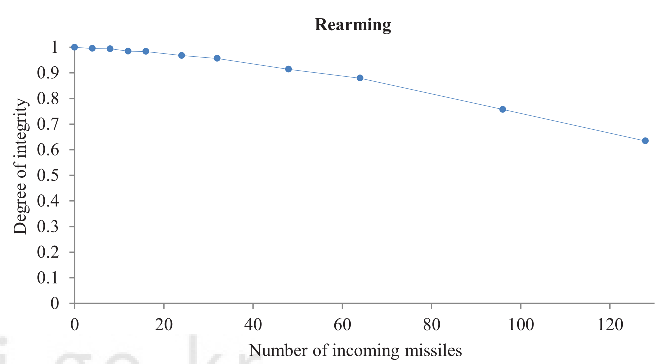

Fig. 16. The degree of integrity of rearming service station.

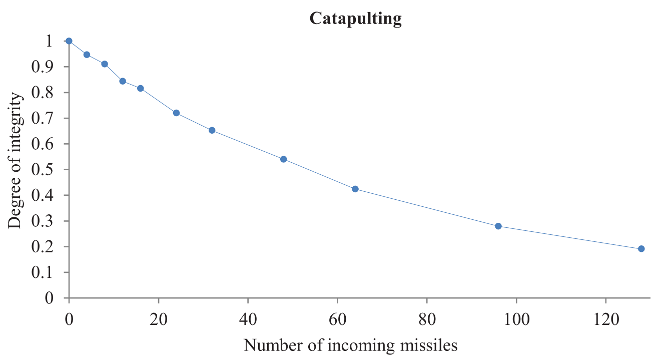

Fig. 17. The degree of integrity of catapulting service station.

128 enemy's anti-ship missiles incoming, the degree of integrity of catapulting service station is less than 0.2. This is mainly because the 4 catapults are very easy to be hit and destroyed by enemy's warheads.

4.2.3. The decline of the sortie and recovery capability

4 representative indexes are chosen to quantificationally evaluate the impact on the sortie and recovery capability, showing in Fig. 18—21, which includes the average of the damaged FPs, the average of the residual aircrafts, the average of the sortie generation rate, and the frequency that the aircraft carrier lose the operational capability. Therein, the situation that the aircraft carrier loses the operational capability indicates that the sortie generation rate is less than 10. Because 10 sorties of an 18-h working day can hardly complete any combat missions for a heavy aircraft carrier and it should retreat from the battlefront in such situation.

From Figs. 20 and 21, it can be inferred that when the incoming enemy's missiles are less than 16, the change rates of these data are relatively mild; the sortie generation rate keeps upon 110 and the probability of losing the operational capability is very small. Thus, the overall operational capability of the aircraft carrier can hardly be weakened by less than 16 missiles. As the number of incoming missiles increases, the data in Figs. 20 and 21 change roughly linearly and the decline of the overall operational capability becomes obvious. By contrast, the number of residual aircrafts in Fig. 19 decreases much slower. When the number of incoming missiles increases

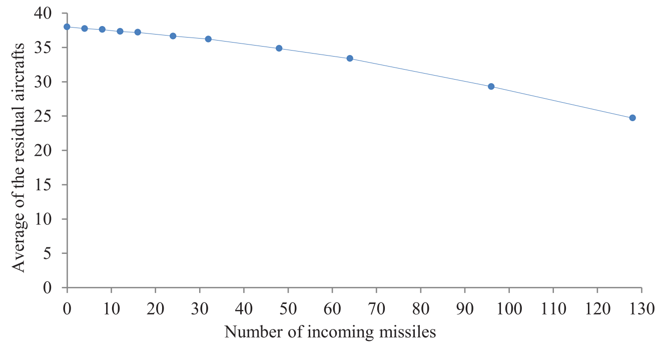

Fig. 19. The change of the average of the residual aircrafts with the different number of incoming missiles.

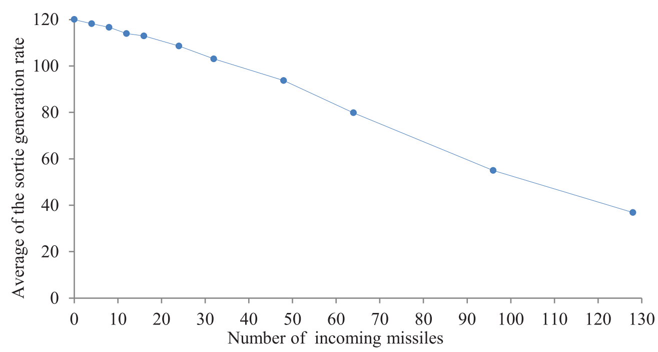

Fig. 20. The change of the average of the sortie generation rates with the different number of incoming missiles.

to 96, there are still about 29 aircrafts able to strike, while the average sortie generation rate is only about 55 according to Fig. 20. This shows that the main reason for the decline of the sortie generation rate is the decrease of the service rates of some service stations caused by some key aircraft guarantee resources being hit by enemy's warheads, rather than the decrease of the residual aircrafts. From Fig. 21, when the enemy employs 128 anti-ship missiles to attack the aircraft carrier, they have nearly half the chance to deprive the aircraft carrier's operational capability, which means such anti-ship firepower can effectively threaten the aircraft carrier. From Fig. 18, it can be inferred that there is no need to destroy the entire flight deck to destroy its working ability and just a

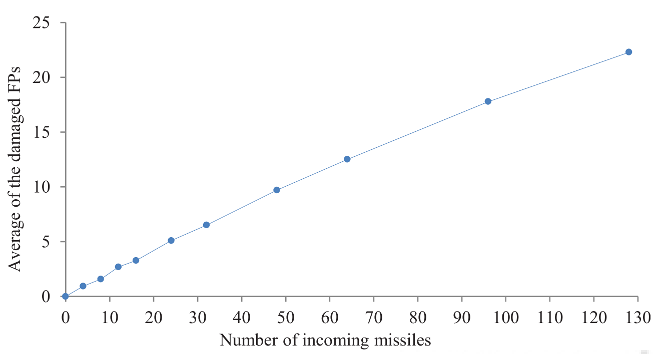

Fig. 18. The change of the average of the damaged FPs with the different number of incoming missiles.

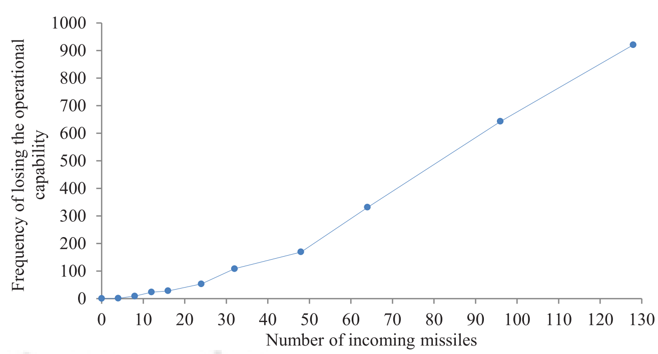

Fig. 21. The change of the frequency of losing the operational capability with the different number of incoming missiles.

number of important FPs being damaged can greatly weaken the aircraft carrier's operational capability, since there are 80 FPs in total.

4.2.4. The possible ways to improve the survivability of the flight deck

On the whole, less than 16 missiles can't do much essential damage to the aircraft carrier's flight deck; if the enemy wants to effectively weaken the aircraft carrier's operational capability, at least 64 missiles are needed; however, only more than 128 missiles may have the chance to totally destroy the aircraft carrier's operational capability. The simulative calculation result shows that even the enemy concentrates all the fire on the flight deck, a heavy aircraft carrier within a strike group still has stronger resistance to the anti-ship missiles than any other kind of surface combat ships.

According to the calculation data, some key FPs or aircraft guarantee resources being destroyed may cause the overall operational capability significantly decline. Thus, the following suggestions may help improve the flight deck's resistance to the anti-ship missiles with cluster warheads:

1) When designing the general arrangement of the flight deck, try to scatter the aircraft guarantee resources and reduce the probability of them being damaged by the same hit.
2) Improve the performance of some aircraft guarantee resources. For example, employ the electromagnetic catapults to replace the steam catapults and this will improve the efficiency and maintainability of the catapult system.
3) Strengthen the maintenance force and increase the storage of the spare parts. For example, increase the establishment of the maintenance crews on the flight deck as well as the relevant devices or increase the storage of spare arresting wires.

5. Conclusions

In this paper, the simulative method to evaluate the aircraft carrier's flight deck's resistance to the attack of the anti-ship missiles with cluster warheads was presented. The result of the case study shows that quite a bit of missiles are needed for the enemy to penetrate through the 3 defense zones of the strike group to effectively weaken the aircraft carrier's operational capability. On the other hand, for the aircraft carrier, even only a little part of the flight deck is damaged, some important aircraft guarantee resources are still possible to be destroyed and this will cause the great decline of the operational capability.

This method may help analyze the sensibility and resistance of the aircraft carrier's flight deck to the anti-ship weapons in the conceptual design period and then provide some technical support for designing the survivability of the aircraft carrier.

Conflict of interest

The authors declared that there is no conflict of interest.

Acknowledgments

This research has been supported by the National Natural Science Foundation of China (NSFC) under Grant Nos.51309061 and 51379040, and the Fundamental Research Funds for the Central Universities under Grant No. HEUCFR150113. The authors also would like to thank the anonymous referees for their valuable comments.

References

Akyildiz, I.F., Gunter, B., 1988. Mean value analysis approximation for multiple server queueing networks. Perform. Eval. 2 (8), 77−91. http://dx.doi.org/10.1016/0166-5316(88)90015-6.

Albert, R., Barabási, A.L., 2002. Statistical mechanics of complex networks. Rev. Mod. Phys. 74, 47−97. http://dx.doi.org/10.1103/RevModPhys.74.47.

Albert, R., Jeong, H., Barabási, A.L., 2000. Error and attack tolerance of complex networks. Nature 406, 378−382. http://dx.doi.org/10.1038/35054111.

Andrieu, C., 2010. Doucet A. Particle Markov chain Monte Carlo methods. J. R. Stat. Soc. 72 (3), 269−275. http://dx.doi.org/10.1111/j.1467-9868.2009.00736.x.

Angelyn, J., 1998a. USS Nimitz and Carrier Airwing Nine Surge Demonstration. Center for Naval Analyses, Virginia, pp. 32−34.

Angelyn, J., 1998b. Sortie Generation Capacity of Embarked Airwings. Center for Naval Analyses, Virginia, pp. 9−95. ADA359178.

Ball, R.E., 1985. The Fundamentals of Aircraft Combat Survivability Analysis and Design, first ed. American Institute of Aeronautics and Astronautics, Inc., New York.

Ball, R.E., 1994. Establishing the fundaments of a surface ship survivability design discipline. Nav. Eng. J. 106 (1), 71−74. http://dx.doi.org/10.1111/j.1559-3584.1994.tb02798.x.

Bryant, R.M., Krzesinski, A.E., Lakshmi, M.S., 1984. The MVA priority approximation. ACM Trans. Comput. Syst. 2 (4), 335−359. http://dx.doi.org/10.1145/357401.357406.

Cornebise, J., 2009. Adaptive Sequential Monte Carlo Methods. University Pierre of Marie Curie, Paris, pp. 45−76.

Dastidar, R.G., Frazzoli, E., 2011. A Queueing Network Based Approach to Distributed Aircraft Carrier Deck Scheduling. AIAA. http://dx.doi.org/10.2514/6.2011-1514.

Dietz, D.C., Jerkins, R.C., 1997. Analysis of Aircraft Sortie with the use of a fork-join queueing network model. Nav. Logist. Res. 2 (44), 153−164. http://dx.doi.org/10.1002/(sici)1520-6750(199703)44, 2<153::aid-nav1>3.0.co;2−8.

Harris, J.W., 2002. The sortie generation rate model. In: The 2002 Winter Simulation Conference, Simulation Conference, USA, pp. 864−868. http://dx.doi.org/10.1109/wsc.2002.1172972.

Michini, B., How, J.P., 2011. A human-interactive course of action planner for aircraft carrier deck operations. In: Proceedings of the AIAA Infotech@ Aerospace Conference. http://dx.doi.org/10.2514/6.2011-1515.

Norman, F., 1983. US Aircraft Carriers. Naval Institute Press, pp. 318−321.

Rains, D.A., 1994. Methods for ship military effectiveness analysis. Nav. Eng. J. 41 (2), 34−37. http://dx.doi.org/10.1111/j.1559-3584.1994.tb02828.x.

Reese, R.M., Calvano, C.N., 1998. Operationally oriented vulnerability requirements in the ship design process. Nav. Eng. J. 110 (1), 19−20. http://dx.doi.org/10.1111/j.1559-3584.1998.tb02383.x.

Reiser, M., 1979. A queueing network analysis of computer communication networks with window flow control. IEEE Trans. Com. 27 (8), 1199−1209. http://dx.doi.org/10.1109/tcom.1979.1094531.

Ryan, J.C., Cummings, M.L., Roy, N., Banerjee, A., 2011. Designing an interactive local and global decision support system for aircraft carrier deck scheduling. In: Proceedings of the AIAA Infotech@Aerospace Conference. http://dx.doi.org/10.2514/6.2011-1516.

Said, M.O., 1995. Theory and practice of total ship survivability for ship design. Nav. Eng. J. 107 (3), 190−191. http://dx.doi.org/10.1111/j.1559-3584.1995.tb03085.x.

Shu, M., Cheng, C., Chang, J., 2006. Using intuitionistic fuzzy sets for fault-tree analysis on printed circuit board assembly. Microelectron. Reliab. 46, 2139−2148.

Sun, S., 2000. Modern Aircraft Carrier. Shanghai Science Popularization Press, Shanghai, pp. 1−20 (in Chinese).

Vassalos, D., 1999. Shaping ship safety: the face of the future. J. Mar. Technol. 36 (2), 61−73.

Wasmund, T.L., 2001. New model to evaluate weapon effects and platform vulnerability: AJEM. Wstiac Newsl. 2, 1−3.

Zheng, M., Huang, S., Wang, C., Wang, Y., 2013. Research on aircraft sortie generation rate using multi-class closed queueing network. VMEIT 2013, 1864−1867 doi: 10.4028. www.scientific.net/amm.380-384.1864.